AJEMA GLOBAL RESEARCH NETWORK

**AMERICAN Journal of Engineering, Mechanics and Architecture**
*Volume 2, Issue 6, 2024 ISSN (E): 2993-2637*

# Development Corrosion Behavior for 2205 Duplex Stainless Steel by Plasma Nitriding in Simulated Body Fluid

**Safa Hussain Ali**
*Department of biomedical engineering, College of engineering,*
*University of Thi-Qar Thi-Qar, 64001, Iraq*
*Safa.hussain.ali@utq.edu.iq*

**Abstract:** Duplex stainless steels have approximately equal amount of ferrite and austenite, due to an accurate control of chemical composition and thermo-mechanical treatment. This phase balance allows the best combination of mechanical and corrosion resistance properties. Alloy 2205 DSS exhibits an excellent combination of both strength and corrosion resistance, the approximate 50/50 ferrite-austenite structure provides excellent chloride pitting and stress corrosion cracking resistance but lack wear resistance. Nitrogen Plasma techniques perform an unrivaled way to improve the surface characteristic of materials used in medical and biology application. This technique is very important used in many industries to change the surface characteristics of the material used in medical applications at different parameter with different parameters at vacuum chamber of air (2mbar), 680 volt and 30 mA .Use different time for plasma nitriding (5, 15 and 25) hrs on the chemical structure of 2205 DSS alloy and the form of phases was investigated using OM, FESEM with EDS, XRD, and antibacterial test, tafel potential polarization and cyclic polarization for biomedical application. The results indicate the formation of layers and phases S, Fe3N, and Fe2-3N were formed on the alloy's surface, which would improve mechanical properties and corrosion resistance in Ringer solution at 37 ◦C.

**Keywords:** 2205 duplex stainless steel, plasma nitriding , corrosion behaviour.

## Introduction

The duplex stainless steels have excellent resistance for corrosion, combined with high strength, with better mechanical strength and higher pitting resistance than austenitic stainless steels. DSS alloys have also SCC resistance better than 316 austenitic stainless steel in chloride contained environment, yield strengths twice than austenitic and impact resistance higher than ferritic ones [1].

The yield strength of DSS is around 400 MPa, while the yield strength austenitic stainless steels is about 200 MPa, this means that the DSS is stronger and harder than austenitic. They have also better performance when abrasion is a concern. Due to these attractive properties and their relatively low cost, the DSS markets and application have increased continuously [2-3]. The addition nitrogen on surface DSS improve their properties. The addition of selective alloying elements such as (Mo, N, Ni and Cr) allowed duplex structure (austenite and ferrite phase) in approximated volume fraction, has took place to these types of SS which have strength higher than austenitic SS, toughness better than ferritic stainless steel, excellent corrosion properties in a many of corrosive media such as pitting, SCC, intergranular corrosion and excellent weldability. The DSS nitride is non toxic coating has appropriate good compatibility with human body has made it a good candidate for coating in medical implant. The aim of the project are evaluate the corrosion behavior of 2205 DSS alloy in simulated body fluid by using plasma nitriding at the different nitride time.[4-5]

## 2.Experimental

### 2.1Materials and Methods

The alloy used in this research is 2205 duplex stainless steel which made in Sweden Outokumpu factory for stainless steel and high performance alloys. These alloys contain Ni less than 316 stainless steel which has advantage in biocompatibility and cost where 2205 less cost than 316 stainless steel. which cut by wire cut machine (knuth smart DEM made in Germany) to a diameter 15mm and thickness 3mm for rod type. The chemical composition of the 2205 DSS alloy is given in table 1. The first step involve the grinding of samples in silicon carbide paper (120, 220, 320, 600, 1000, 1200, 2000, 2500 and 3000 grit), after that these samples were rinsed by distilled water, then polished by using a polishing cloth with diamond suspension of (9, 3,1) μm to gat bright mirror finish. After polishing sample, then ultrasonically cleaned with ethanol medium for 10 min, to remove any impurities from surface, then dried the sample by steam air. The solution for etching was prepared by adding 40 g of sodium hydroxide (NaQH) to 100 ml of distilled water (H2O) at 2V dc bower with platinum electrode where the samples was positive or anode electrode . After 10 seconds of etching process (emersion time) , then wished the sample in water and followed by air drying.

**Table 1 chemical composition of 2205 DSS Alloy**

| 2205 DSS alloy | UNS | Cr | Ni | Mo | C | N | Fe |
|---|---|---|---|---|---|---|---|
| | S32205 | 22.6 | 5.8 | 3.1 | 0.016 | 0.201 | balance |

### 2.2 Surface modification by plasma nitriding

The clean samples after grinding and polishing are placed on the anode desk made of stainless steel in the center of the dark shield the diameter of up electrode is 14.5cm as shown in Figure 1. a target (cathode) is connected to the DC power supply is shielded by insulator disk made of Ceramic and stainless steel holder, the diameter of dark catholic space is 7.5 cm and the gap distance between two electrode can be varied from 4 to 6 cm and in the Durant study 4cm gap distance used, which provides an electrical filed for the gas to be discharge. After vacuum chamber by using high vacuum system consist of rotary and torbo-molecular vacuum pump feel the chamber in N gas for glow-discharge plasma nitriding, the parameters are given in Table 2. After the process was finished, switch off voltage dc power supply and aeration the chamber in nitrogen gas to purpose reduce the pressure inter the vacuum chamber and exit the samples.

**Table 2 Plasma nitiding parameter for 2205 DSS alloy**

| Materials | Fixed condition | Time operation |
|---|---|---|
| 2205 DSS alloy | DC voltage =680V | 5, 15 and 25 hrs |
| | Total pressure =2mbar | |
| | Discharge current=30mA | |
| | Source gas = nitrogen | |

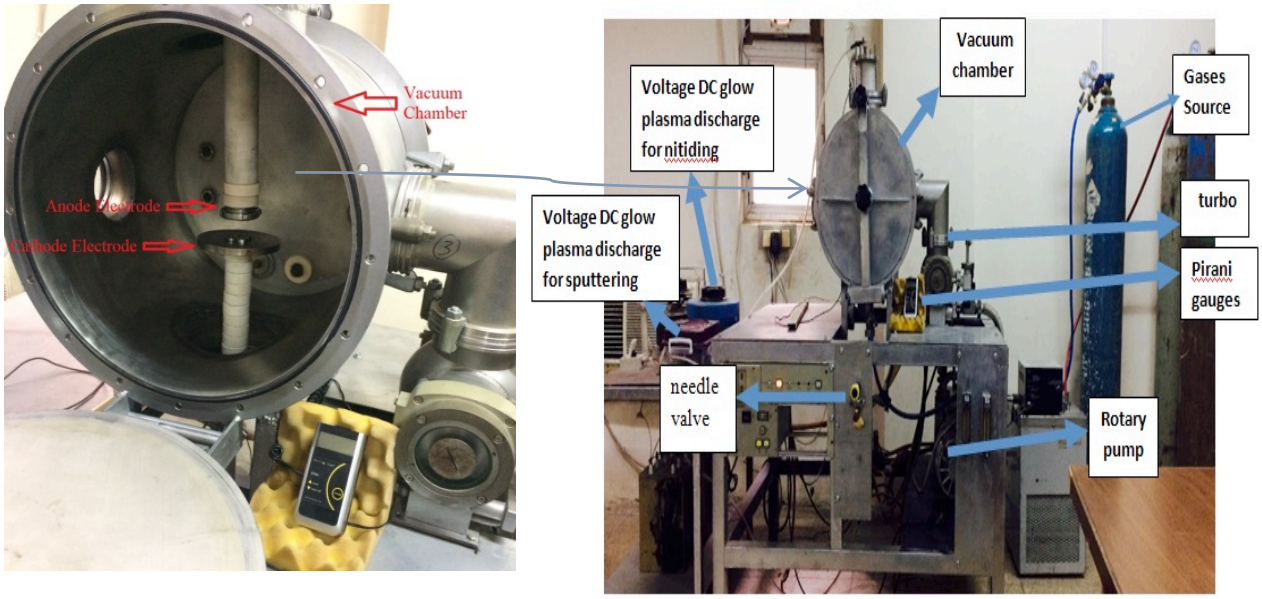


**Fig. 1 the plasma ntriding system**

### 2.3 Metallographic Characterization of plasma nitriding samples

The aim main of using the optical microscopy to detect the ferrite and austenite phases (shape and distribution) . the Optical microscope examination was done by using (NMM-800RF, made in Chine) Digital Camera DXM 1200F microscopy made in Chine ,with magnification (X500-X1000). . the surface morphology observed by using the SEM, SESEM ZEES type microscopy at different parameter, and determination the depth and thickness of the nitride zone as well as the average grain size related to the plasma process. X-ray diffraction (The Shimadzu Lab X XRD-6000, Japan) used in this study to know the phases formation during plasma nitriding. The test accomplished by using copper target(Kα radiation = 1.5418$A^O$) with nickel filler. The scanning speed of the diffractmeter was adjusted to $6^O$ per minute with the range of the diffraction angle 2θº was (20º-80º).

### 2.4 Rockwell hardness test(Adhesion test)

The adhesion was measured with Rockwell hardness test type- C, and according to ASTM E 384 – 99 (standard test method for micro hardness of Materials)[ 6]. It uses of a standard Rockwell hardness fit by Rockwell (type- C ) Diamond cone by an applied (150 kg). Rockwell hardness test carried out on duplex stainless steel before and after plasma nitriding.

### 2.5 Electrochemical corrosion test

There are two types of corrosion tests have been carried out in this study. The first one is potentiodynamic polarization were used as the method to determine general corrosion behavior for 2205 DSS alloy and cyclic potentiodynamic polarization method was used to identify the pitting behavior of the 2205 DSS alloy. All samples of 2205 DSS alloy prepared and coating by plasma nitriding process at different time. The corrosion behavior for all sample studied in ringer solution of 500ml at 37ºC. The test was carried out at 0.4 mV/s from an initial potential of 200 mV above the open circuit potential and the scan continued up to 200 mV under the open circuit potential. The potentiodynamic polarization cell , included the WE= working electrode, RE= reference electrode (saturated calomel electrode and CE =counter electrode (platinum).

## 3.Results and discussion

### 3.1 microstructure and morphology observation

The microstructure of the 2205 DSS as in Figure 2 which show that the microstructure for untreated specimen contains only ferrite and austenite and no secondary phases were observe.

The ferrite appears darker than the austenite on the micrograph. Quantitative analysis of the microstructure using MIP4 student material program gave an area fraction of 50.5% ferrite and 49.5% austenite. which is in agreement with reference[7]

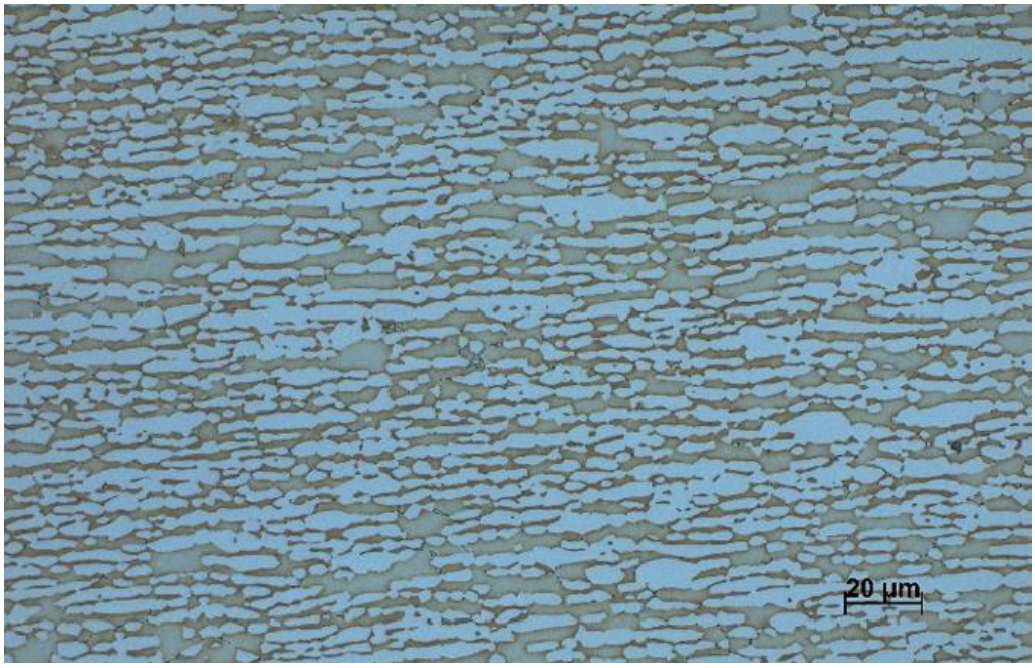


**Fig.2 The Optical micrographs of 2205 duplex stainless steel, with ferrite (dark) and austenite (light) phases.**

In Figure 3 a, b and c, the cross section morphology of plasma nitriding of 2205 DSS alloy for 5, 15 and 25 h nitriding time is observed by emission scanning electron microscopy . the nitride layer that formed on the surface substrate uniform , comprehensive adhesion between the ntride layer and substrate and there was no gap between the coating and surface substrate. Coating layer thickness usually increase as the nitriding time increased. When nitriding over 15 hrs. the thickness of nitride layer at 5 hrs was 27.32 nm and for 15h was 48.7 nm and for 25h was 33.67nm , the thickness decreases slowly, The reason for this is that as the nitriding time is extended, the number of nitrides formed on the surface of 2205 DSS increases, resulting in increased nitrogen diffusion resistance and decreased nitride formation ability [8]. Some cracks were observed on the surface nitride layer when the nitride time between 15 and 25 hrs This may be due to the fact that as the nitriding time increases, the brittle phase of CrN increases and coarsens, causing the surface layer's toughness to decrease. Furthermore, the structural variations between the phases in the surface layer increase residual stress [8-9].

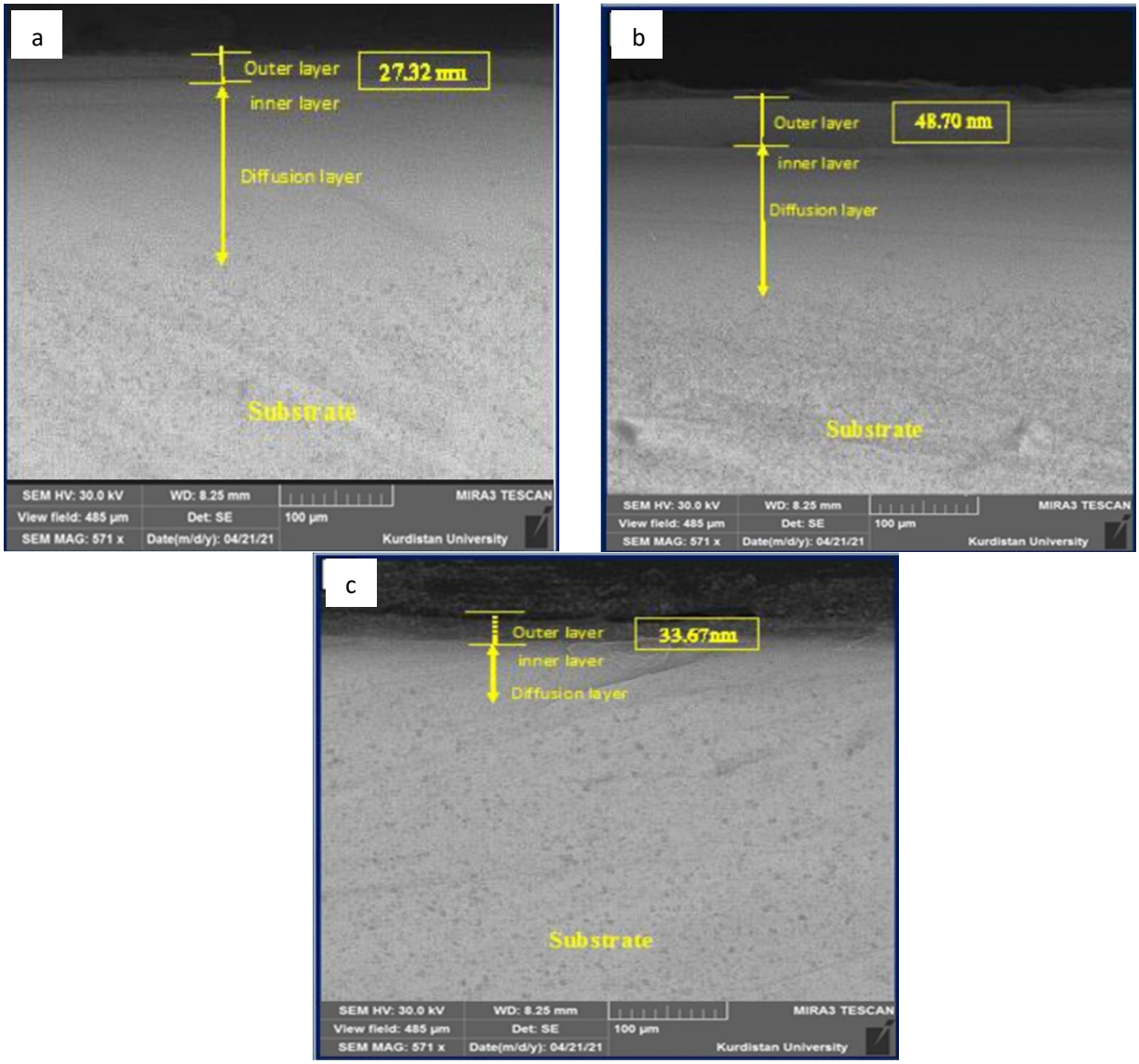


**Fig. 3 FESEM micrographs of the cross section for plasma nitrided 2205 DSS alloy for a) 5 hrs , b) 15 hrs, c) 25 hrs**

### 3.2 Chemical compassion distribution of phases

The concentration of major alloying element in the ferrite and austenite phases were determent by EDS ( energy dispersive X-ray spectroscopy) before and after plasma nitriding . Diffraction pattern for 2205 DSS alloy before treatment the Figures 4 show the peaks corresponding to ferrite and austenite phase only. But after plasma nitriding at different time greatly effected on concentration element in each alloy , which have significant effect on corrosion behavior on each alloy

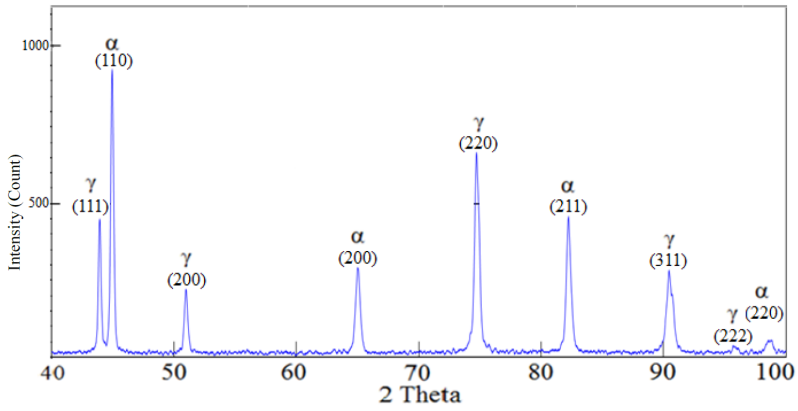


**Fig.4 X-Ray diffraction pattern of 2205 DSS specimen before nitride**

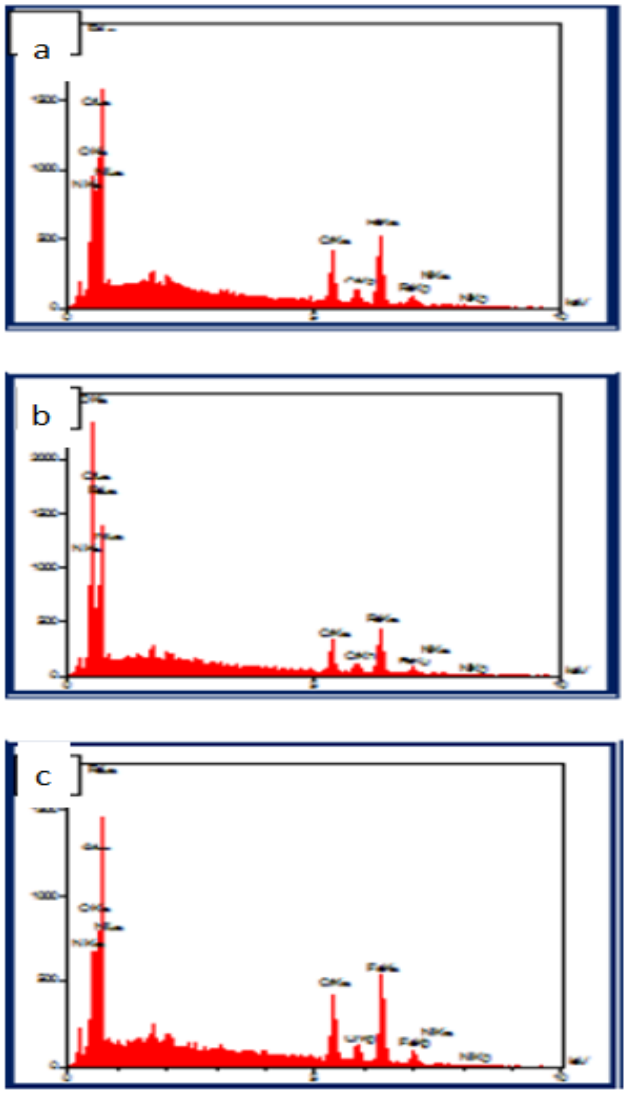


**Fig. 5 EDS for nitrided samples at condition: (R) untreated (a) 5, (b) 15 and (c) 25 hrs.**

The main elements of Fe, Cr, N, and Ni are found in the nitriding layers, as can be observed in figure 5. These elements confirm the successful formation of a nitrided surface on the 2205 DSS alloy. Moreover, there is no other Peaks different from nitride and this assure the coating purity. Table.2 illustrates these elements percent for each sample.

**Table 3 elements present of nitriding layer on 2205 DSS alloy**

| No | Condition | Fe% | Cr% | Ni% | N% |
|---|---|---|---|---|---|
| a | 5 hrs | 62.6 | 21.6 | 5.50 | 2.98 |
| b | 15 hrs | 53.9 | 18.35 | 6.35 | 3.50 |
| c | 25 hrs | 63.35 | 23.67 | 6.70 | 2.60 |

### 3.3 Phase adentiffication of 2205 DSS alloy

The prescience phases were identified using XRD research. Figure 6 displays the sample's diffraction patterns before nitriding, revealing that the peaks only refer to phases of austenite and ferrite. Figure 4 also shows an XRD diffractograph of samples using standard JCPDS-ICDD (Joint Committee on Powder Diffraction Standards—International Center for Diffraction Data) standards. The XRD results, (Fig.6), revealing crystalline α and γ phases in the reference (untreated) 2205 DSS sample, these phases are identified with their crystalline planes according to the JCPDS card numbers where the diffraction pattern of the ferrite phase match with the (JCPDS Card No. 06-0694) peaks and the austenite phase match with the (JCPDS Card No. 33-0397). In all of the surfaces after nitriding, the N (expanded austenite - S-phase) and nitride (-Fe4N and -Fe2-3N) phases were identified. Similarly, as the treatment time increased, the α phase of plasma nitrided DSS converted into γN, Ɛ-Fe2-3N, and Ɛ + CrN, the γN phase being the main phase on the surfaces in accordance in the literature [9 - 11].

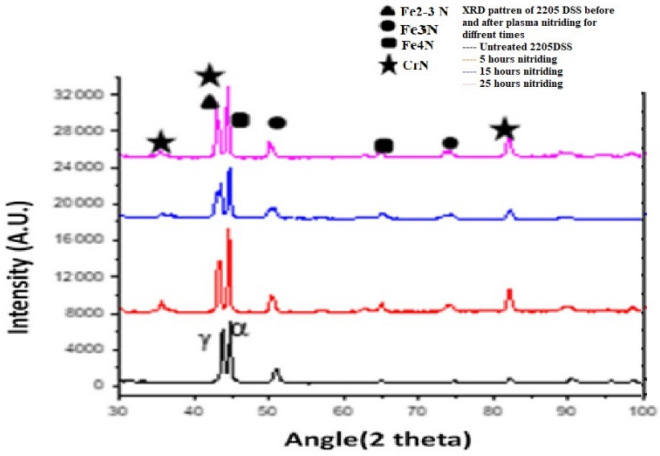


**Fig.6 XRD Patterns of 2205 DSS alloy before and after plasma nitriding at different times**

### 3.4 Adhesion test

The hardness values mainly depend on the presence or absence of coating layer because it is brittle and hard. The bulk hardness depends on phases fraction in which indentation occurs.as shown in Figure 7. The results demonstrate that these samples' adhesion strength quality is related to HF1 and HF2 but also radial cracking, and these defects are classified as HF2–HF3 adhesion strength quality. The adhesion of all nitrided samples is acceptable, while the substrate has poor adhesion, in the nitride samples seen the deep and long cracks seen indentation point.[12-14]

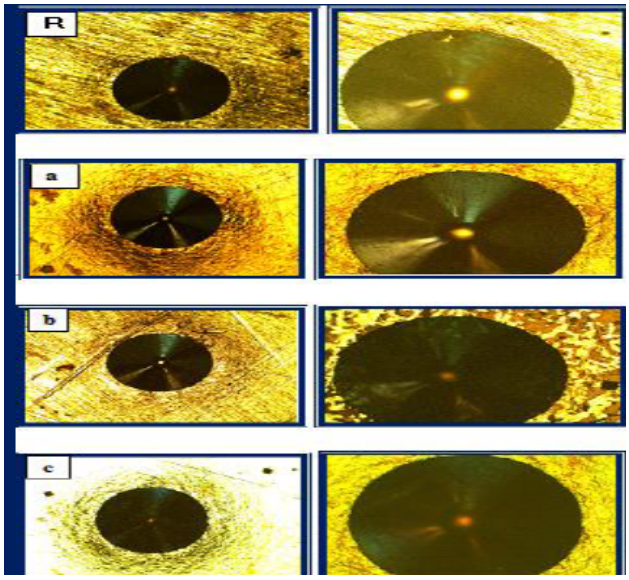


**Fig.7 Optical photography of Rockwell hardness test type- C for nitride samples all deffrint condition R. untreated, a, 5 h nitriding, b. 15h nitriding , c.25h nitriding**

### 3.5 Electrochemical corrosion behavior of 2205 DSS alloy

The electrochemical behavior of the experimental alloys was compared before and after plasma nitriding of 2205 DSS and was investigated by the Tafel potentiodynamic polarization method in a simulated body fluid at 37 °C. The main parameters that can be obtained from these curves are the current density (icorr) and potential (Ecorr) for interment of the 2205 DSS alloy at different conditions. These results are in agreement with the findings led by Yildiz et al. [8], Shown in table 4 and figure 8, the in which they investigate the corrosion current density decrease from 1.75 µm/cm2 for Untreated sample and1.24 µm/cm2 for 5 hour and 0.85 µm/cm2 for 15 hour, the untreated alloy has high current density but after nitriding provide the protective layer on the spaceman layer that while reduce the current density and reduce the corrosion rate. when nitride of 5 and 15 hour good corrosion resistance lowest current density. While, the 25 hours showed some micro crack in the structure and the percent the CrN in structure this lead to reduce the corrosion resistance. This result indicates that the compound layer formed on the surface contains pores and rough surface, which increase with increasing nitriding time, therefore corrosion resistance was reduced. Figure 8 details the comparison for the current density of untreated and plasma-nitrided alloys at different nitriding times. Corrosion resistance of 2205 DSS is higher than the common biomedical austenitic SS (316L) when they are immersed in the physiological solutions as Ringer's, as mention in literature review, which means less toxicity and consequently the implant life is expected to be higher. Finally, as the nitriding time increases, the diffusion layer increases corrosion resistance, but after 15 hours of nitriding, the uptrend remains stable [15-17].

**Table 4 corrosion current (Icorr) and corrosion potentials (Ecorr) of 2205 DSS alloy plasma nitriding for 5, 15 and 25 hours comparison to untreated**

| Condition | Icorr $*10^{-3}$ Ma/Cm2 | Ecorr Mv | Corrosion Rate (Mpy) |
|---|---|---|---|
| untreated | 1.75 | -34.2 | 0.329 |
| 5 hrs | 1.24 | -104.1 | 0.203 |
| 15 hrs | 0.85 | -37.4 | 0.175 |
| 25 hrs | 4.26 | 10.2 | 2.257 |

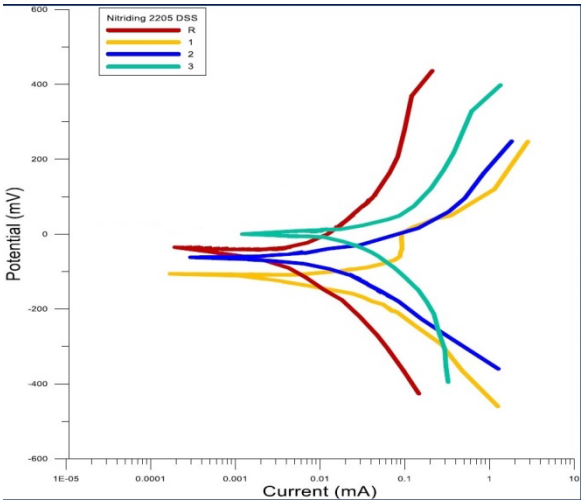


**Fig. 8 Electrodynamics polarization for untreated and plasma nitridining of 2205 DSS alloy at different condition R) untreated, 1) 5h N, 2) 15 hN and 3) 25hN**

whereas in the lower nitriding time, the N concentration in the Fe layer will be not enough to form nitride compound and N will be in the solid solution which is freer to form with O (from the solution) oxynitride compound and this compound will be in the form of fine precipitates enhancing the alloy tendency to passivity. Clearly, the high time nitrided samples had lower corrosion resistance than the untreated samples (due to CrN formation and Cr depletion in the surrounding areas), whereas the low time treated samples had higher corrosion resistance [8].

### 3.6 Cyclic Polarization of Plasma Nitriding

The biocompatibility performance of the 2205 DSS alloy is closely associated with its corrosion resistance and the biocompatibility of its corrosion products. The 2205 DSS alloy shows excellent corrosion resistance, even though precautions should be taken in order to optimize the products composition. In addition to uniform corrosion, the 2205 DSS alloy when exposed to an aggressive environment can undergo localized corrosion in which the passive layer breaks down locally leading to the formation of pits[18]. In the case of biomaterial applications, this kind of failure can take place under special conditions such as local infections, surgical trauma, and the like. Therefore, it is very important to evaluate this alloy's susceptibility to localized corrosion, which can be determined by means of anodic cyclic polarization curves especially after nitriding as shown in Fig. 9. The electrochemical behavior of 2205 duplex stainless steel in artificial saliva before and after plasma nitriding were analyzed by cyclic Potentiodynamic polarization. The pitting potential (Ep) or breakdown potential of pitting corrosion (Eb) is the potential above which pits nucleated and grown. The protection potential (Eprot) is the noblest potential where pitting and crevice corrosion will not propagate and at which re-passivation occurs or it is the potential at which the reverse scan intersects the forward scan at a value that is less noble than Ep. ΔE (Ep − Eprot) represents the corrosion resistance of the materials and the smaller the ΔE value is the better the anti-corrosion property. microstructure on the pitting corrosion behavior can be noted by cyclic potentiodynamic polarization. From comparing of the polarization curves of the samples as shown in Figure 9 The difference (ΔE) between Ep and Eprot will give an indication to the corrosion resistance of the sample, where the smaller ΔE value mean the highest corrosion resistance. It is cleared from Fig.9 that the nitrided sample at 25 hrs had the lowest pitting or break down potential and thus low resistance to the pitting corrosion, this is due to the increasing of coarse particles. However, the nitrided sample at 15 hrs has highest pitting and protection potential with a close hysteresis loop where this polarization behavior tends to be resistance to the localized corrosion. In addition, the lowest value of ΔE as shown in table.5 is obtained and consequently this sample would have the more resistance to pitting corrosion. This means that the pit initiation and propagation have been effectively hindered by this sample. Moreover, the nitriding layer have the ability to exhibit efficacious chemical barriers against metal ions release from the metallic implants. Thus, the osseointegration properties could be

improved and the composite coating on 2205 DSS could be used as a biofilm for orthopedic implant applications.[19-20]

**Table 5 Electrochemical parameters of 2205 DSS before and after plasma nitriding obtained in ringer solution at 37°C solution with cyclic polarization**

| Condition samples | Ep(mv) | Eprot(mv) | ΔE (Ep-Eprot) mv |
|---|---|---|---|
| untreated | 694 | -75 | 769 |
| 5 hrs | 780 | 10 | 770 |
| 15 hrs | 710 | -30 | 740 |
| 25 hrs | 696 | -110 | 806 |

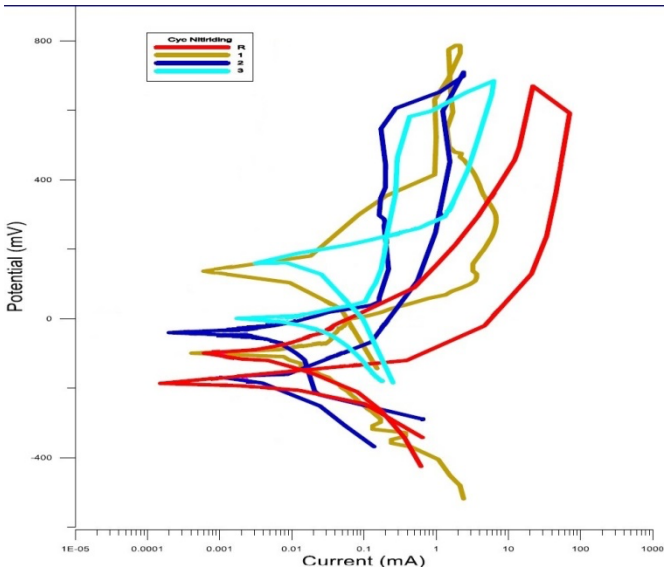


**Fig.9 Cyclic polarization curves for for untreated and plasma nitridining of 2205 DSS alloy at different condition R) untreated, 1) 5h N, 2) 15 hN and 3) 15hN**

## Conclusion

1. Plasma nitriding affects the base duplex stainless steel phases of ferrite and austenite differently. The initial austenite grains in the surface of the 2205 DSS form the S-phase (expanded austenite) as plasma nitrided at low temperatures, whereas "Fe3N" was precipitated from nitrogen saturated ferrite grains.
2. Elemental analysis by EDS and SEM micrographs show that the formation thickness of a nitride layer on the surface of the 2205 DSS alloy increases with an increase in plasma nitriding times 5 and 15 h and thin decrease at 25 hours.
3. XRD studies showed the formation of nitrides (Fe3N, Fe2-3N), whereas increasing of nitriding times at 25 hrs leads to the formation of CrN.
4. The results obtained from polarization curves suggest that the plasma-nitrided Ti–6Al–4V alloy for different nitriding times improved corrosion resistance in a SBF when compared with the untreated alloy. These improvements can be seen from the low current density and low passive current density obtained at 15-h nitriding.

## References


1. Mahajan, Amit, Sandeep Devgan, and Dinesh Kalyanasundaram. 2023,"Surface alteration of Cobalt-Chromium and duplex stainless steel alloys for biomedical applications: a concise review." Materials and Manufacturing Processes 38.3 pp. 260-270.
2. S. Arango Santander and C. M. Luna Ossa, 2015, “Stainless Steel: Material Facts for the Orthodontic Practitioner,” Rev. Nac. Odontol. vol. 11, no. 20.

3. Mohamed, A. Y., Mohamed, A. H. A., Abdel Hamid, Z., Farahat, A. I. Z., & El-Nikhaily, A. E. (2023). Effect of heat treatment atmospheres on microstructure evolution and corrosion resistance of 2205 duplex stainless steel weldments. Scientific Reports, 13(1), 4592
4. A. S. Hammood, L. Thair, and H. Ali, 2019, "Corrosion Behavior Evaluation in Simulated Body Fluid of a Modified Ti–6Al–4V Alloy by DC Glow Plasma Nitriding," vol. 5, no. 4, pp. 1–8.
5. Aghajani H, Behrangi S (2016) Plasma nitriding of steels, 1st edn. Springer, Cham
6. ASTM (2005) Designation: E 384-99 standard test method for micro hardness of Materials. ASTM, West Conshohocken, PA
7. Yan, J., Wang, J., Lin, Y., Gu, T., Zeng, D., Huang, R., & Fan, H. (2014). Microstructure and properties of SAE 2205 stainless steel after salt bath nitrocarburizing at 450 C. Journal of materials engineering and performance, 23, 1157-1164.
8. J. Yan, T. Gu, S. Qiu, J. Wang, J. Xiong, and H. Fan, 2015, "Phase Transformations During the Low- Temperature Nitriding of AISI 2205 Duplex Stainless Steel," Metall. Mater. Trans. B Process Metall. Mater. Process. Sci., vol. 46, no. 3, pp. 1461–1470.
9. S. N. Kane, A. Mishra, and A. K. Dutta, 2016, "Preface: International Conference on Recent Trends in Physics (ICRTP 2016)," J. Phys. Conf. Ser., vol. 755, no. 1.
10. Li, X. Y., Roberts, R., Dou, W. B., & Dong, H. S. 2014. Low temperature plasma surface alloying and characterisation of a superduplex stainless steel. International Heat Treatment and Surface Engineering, 8(2), 61-64.
11. K. Taherkhani and M. Soltanieh, 2019, "Investigation of nanomechanical and adhesion behavior for AlN coating and AlN/Fe2-3N composite coatings created by Active Screen Plasma Nitriding on Al 1050," J. Alloys Compd., vol. 783, no. April, pp. 113–127.
12. Y. Kayali and S. Taktak, 2015, "Characterization and Rockwell-C adhesion properties of chromium-based borided steels," J. Adhes. Sci. Technol., vol. 29, no. 19, pp. 2065–2075.
13. Al-Murshdy, J. M. S., Hammood, A. S., & Fahad, N. D. (2021, August). Improvement corrosion behaviour of lean duplex stainless steel 2101 alloy in ringer solution by plasma nitriding for biomedical applications. In Journal of Physics: Conference Series (Vol. 1973, No. 1, p. 012070). IOP Publishing.
14. Mphahlele, M. R. 2018. Mechanical and tribological properties of nanoceramics ispersion strengthened 2205 duplex stainless steel. University of Johan
15. Borges, F. M. R., Borges, W. F. A., Santos, R. L. P., Leal, V. S., Santos Júnior, J. R. D., Lobo, A. O., & Sousa, R. R. M. D. 2021. Corrosion Resistance and Microstructural Evaluation of a Plasma Nitrided Weld Joint of UNS S32750 Super Duplex Stainless Steel. Materials Research, 24, e20210087.
16. W. Ye and X. S. Tong, 2014, "Effect of Atmosphere Proportion and Nitriding Time on Plasma Nitriding of Duplex Stainless Steel," Adv. Mater. Res., vol. 1061–1062, pp. 61–64.
17. Dan, N. E., Hussain, P. B., Shaik, N. B., Bakthavatchalam, B., Mohapatra, R. K., & Behera, A. 2022. Improved surface morphology and corrosion resistance performance of 2205 duplex stainless steel by low temperature gas nitriding. Journal of Bio-and Tribo-Corrosion, 8(4), 100
18. T. Bellezze, G. Giuliani, and G. Roventi, 2018, "Study of stainless steels corrosion in a strong acid mixture. Part 1: cyclic potentiodynamic polarization curves examined by means of an analytical method," Corros. Sci., vol. 130, pp. 113–125.
19. Jirarungsatian C, Prateepasen A, 2010, 'Pitting and uniform corrosion source recognition using acoustic emission parameters'. Corros Sci 52:187–197

20. Shen, H., Wang, L., & Sun, J. (2021). Effect of plasma nitriding at low temperature on the corrosion resistance and conductivity of 2205 duplex stainless steel. Surface Engineering, 37(6), 749-754.